IEEE Access
Multidisciplinary | Rapid Review | Open Access Journal

Received March 15, 2019, accepted April 2, 2019, date of publication April 9, 2019, date of current version April 25, 2019.

Digital Object Identifier 10.1109/ACCESS.2019.2909771

Integration Design of Millimeter-Wave Filtering Patch Antenna Array With SIW Four-Way Anti-Phase Filtering Power Divider

HUAYAN JIN[1], (Member, IEEE), GUO QING LUO[1], (Member, IEEE), WENLEI WANG[1], WENQUAN CHE[2], (Senior Member, IEEE), AND KUO-SHENG CHIN[3], (Senior Member, IEEE)

[1]Key Laboratory of RF Circuits and System, Institute of Antennas and Microwave Technology, Ministry of Education, Hangzhou Dianzi University, Hangzhou 310018, China
[2]School of Electronic and Information Engineering, South China University of Technology, Guangzhou 510641, China
[3]Department of Electronic Engineering, Chang Gung University, Taoyuan 333, Taiwan

Corresponding author: Guo Qing Luo (luoguoqing@hdu.edu.cn)

This work was supported in part by the Zhejiang Provincial Natural Science Foundation of China under Grant LQ18F010003, and in part by the National Natural Science Foundation of China under Contract 61722107.

ABSTRACT In this paper, the integration design of a millimeter-wave filtering patch antenna array fed by a substrate integrated waveguide (SIW) four-way anti-phase filtering power divider is proposed. The multilayer four-way anti-phase filtering power divider handily implemented using the intrinsic field distribution of TE_{20}-mode in SIW is proposed for miniaturization. The signal of the lower substrate integrated waveguide cavity (SIWC) bandpass filter is directly coupled to the upper TE_{20}-mode SIW through a coupling slot. The intrinsic field distribution of TE_{20}-mode SIW is used to generate anti-phase signals. This filtering power divider can be utilized as the feeding structure of a millimeter-wave filtering antenna array. To verify the design concept, a 28-GHz SIW-fed 1 $\times$ 4 filtering patch antenna array with three-layer substrates is designed and fabricated. The measured results show a fractional bandwidth of 5.03% ranging from 27.15 to 28.55 GHz, a peak gain of 11.1 dBi, cross-polarization levels lower than -20 dB, symmetric radiation patterns in both *E*-plane and *H*-plane, and high selectivity.

INDEX TERMS Dual-slot-fed patch, filtering antenna array, millimeter-wave antenna array, substrate integrated waveguide (SIW), TE $_{20}$-mode.

I. INTRODUCTION

The rapid development of modern wireless and mobile communication industries proposes stringent requirements on the RF front-end systems with compact size, high-efficiency and good stability. Multifunctional components such as balun bandpass filter [1], filtering power dividers [2], and filtering antennas [3], [4], have received increasing attentions due to their advantages of compact size and low insertion loss. Traditionally, the bandpass filter and antenna, which are two key components in the RF-front ends, are designed individually and then combined by matching networks. This design is not appropriate to circuit miniaturization and will add extra insertion losses. Filtering antennas, which combine the separated antenna and filter into one, can perform filtering response in both the reflection coefficient and realized gain, for size and loss reduction.

The associate editor coordinating the review of this manuscript and approving it for publication was Xiaojie Su.

There have been extensive investigations on filtering antennas [3]–[7]. In [3], one filtering antenna, also called as ''filtenna'', is constructed by a horn antenna and an X-band bandpass frequency selective surface. A high-gain filtering patch antenna operating at the band of LTE (Long term evolution) without extra filtering circuits was presented in [4]. In [5], one X-band filtering aperture antenna array was designed using rectangular waveguide structures. Three-dimensional filtering slot antenna realized at Ka-band using substrate-integrated waveguide (SIW) technique was proposed in [6]. In [7], an SIW-based circularly-polarized filtering patch antenna array was proposed around X-band. Although the above filtering antennas achieve good filtering response, few of them operate at millimeter-wave (MMW) band.

Power dividers, especially multi-way power dividers, are indispensable parts to the design of antenna arrays. Various multi-way power dividers were presented in [8]–[10].

Bandpass filter is another important device in RF systems to reject unwanted signals. These two devices are generally cascaded in the feed networks of antenna arrays. This is the simplest method to construct a filtering power divider, but often at the cost of increasing the size and degrading the in-band performance of antennas. To overcome such shortcomings, the designs of filtering power dividers with low insertion loss, compact size, and low cost were developed [11]–[13]. However, most of the previous works are based on microstrip structures, which may suffer from high insertion loss in MMW systems. SIW structures featuring low insertion losses and high power handling capacities have been widely used in various MMW circuits [14]–[16]. However, SIW power dividers with multi-ways have the disadvantages of large size due to an increased number of ports, and may suffer with poor impedance matching at all ports [9]. The development of MMW SIW multi-way filtering power divider and its application are rarely reported. Because of the influence of small size and serious parasitic effects on MMW antenna designs, how to combine the filtering, power-dividing, and radiating structures into antennas for achieving multifunction is challenging. At present, the frequency bands of the published filtering antenna designs were mostly below 6 GHz. Very few MMW-band antenna arrays with the differential feed network were developed for filtering response, high gain, low cross polarization, and symmetric radiation patterns, which are the focus of this work.

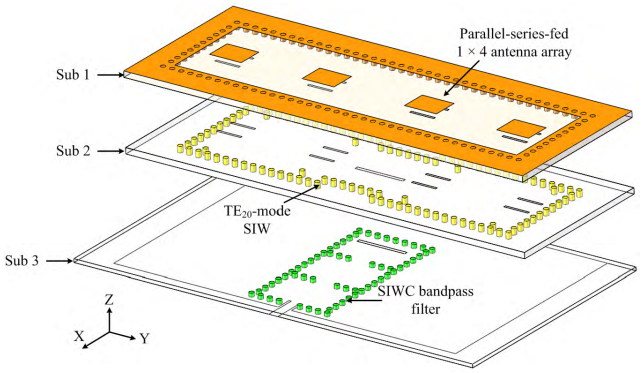

FIGURE 1. 3-D view of the proposed millimeter-wave filtering patch antenna array.

In this paper, the integration design of a MMW filtering patch antenna array is proposed, as shown in Fig. 1. It consists of a novel compact SIW four-way anti-phase filtering power divider and two series-fed 1 × 2 patch antenna sub-arrays. The proposed SIW filtering power divider is handily implemented using the opposite current directions along a coupling slot and the intrinsic field distribution of TE_{20} mode SIW to achieve compact size. It also achieves excellent filtering characteristic, impedance matching at all ports, and amplitude balance at the output ports by integrating a SIWC (SIW cavity) bandpass filter and TE_{20}-mode SIW feed lines. This power divider can directly connect the sub-arrays through TE_{20}-mode SIW without any impedance matching networks. The implemented filtering antenna array shows superior filtering response, flat in-band gain curve, and high out-of-band suppression.

II. FOUR-WAY ANTI-PHASE SIW FILTERING POWER DIVIDER

As it is well known, the differential circuits have the ability to reject common-mode noise compared to single-ended circuits. Furthermore, differential-fed antennas can also reduce cross polarization and improve radiation pattern symmetry [17]. For the design of differential-fed antenna arrays, the anti-phase feed network is required.

In conventional SIW-based structures, an anti-phase filtering power divider is composed by cascade connection of power dividers, bandpass filters, and phase shifters, which will suffer from high loss, large size, and complexity. A compact multilayer four-way anti-phase power divider handily implemented a coupling slot and the intrinsic field distribution of TE_{20} mode SIW is proposed in this work.

A. ANALYSIS AND DESIGN

Fig. 2 shows the configuration of the proposed SIW four-way anti-phase filtering power divider. It consists of a coupling slot, a third-order TE_{110}-mode SIWC bandpass filter, a TE_{20}-mode SIW, and microstrip feed lines. The coupling slot, SIWC bandpass filter, and TE_{20}-mode SIW are implemented together to obtain filtering response and four-way anti-phase outputs. Note that the four output ports of Port

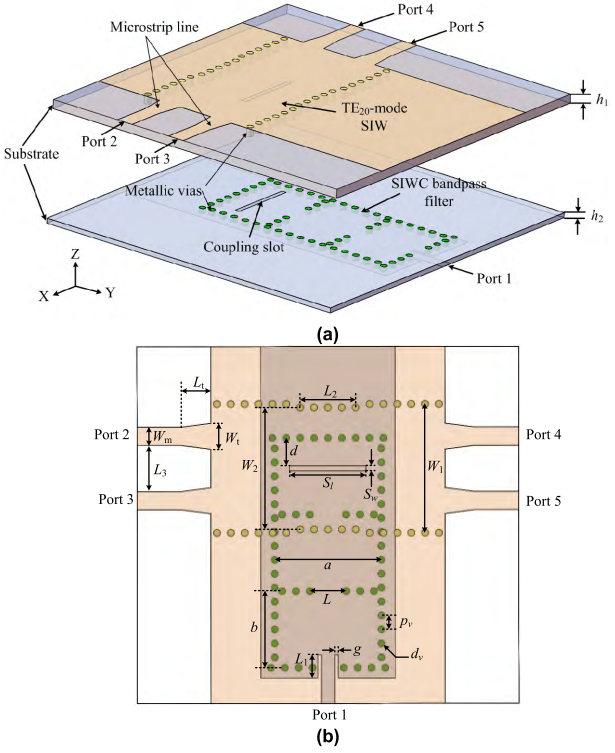

FIGURE 2. Configuration of the proposed SIW four-way anti-phase filtering power divider: (a) 3-D view and (b) Top view.

2−Port 5 are used only for the performance evaluation, which can be removed in the final array design. The $|S_{21}|$ 3-dB bandwidth ranging from 27.22 to 29.15 GHz is designed in this work for 5G wireless applications, which requires a fractional bandwidth of 6.8%. When selecting a third-order maximally flat response and fractional bandwidth of 6.8%, the corresponding coupling coefficients and external quality factor for the SIWC bandpass filter are $M_{12} = M_{23} = 0.048$ and $Q_e = 14.71$, respectively, where M_{ij} is the coupling coefficient between the ith and jth cavities. Fig. 3 shows the design curve of coupling coefficient of the SIWC bandpass filter, which can be used to determine the window length L according to the required M_{ij}.

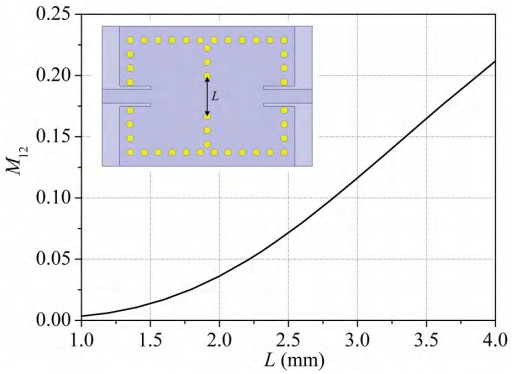

FIGURE 3. Coupling coefficient of the SIWC bandpass filter.

The power divider is designed with two-layer substrates and optimized by the full-wave EM simulator Ansoft HFSS. The Rogers 4003C ($\varepsilon_r = 3.55$ and $\tan\delta = 0.0029$ at 10 GHz) with a thickness of 0.5 mm was used for the upper TE_{20}-mode SIW, while the Rogers RT/Duroid 5880 ($\varepsilon_r = 2.22$ and $\tan\delta = 0.0009$ at 10 GHz) with a thickness of 0.254 mm was used for the lower SIWC bandpass filter. A common ground plane with a coupling slot was inserted between the two substrates. The input signal from Port 1 propagates along the third-order SIWC bandpass filter, and then is directly coupled to the upper TE_{20}-mode SIW from the third resonant cavity without any additional structures and equally divided into two TE_{20}-mode signals. The coupling slot located along the longitudinal center of the TE_{20}-mode SIW line is in charge to generate the TE_{20}-mode field distribution. The intrinsic field distribution of TE_{20}-mode in SIW can be used to construct four-way anti-phase signals.

The SIWC bandpass filter is constructed by three SIW cavities operating at the TE_{110} dominant mode, whose resonant frequency can be determined by [18]:

$$f_{110} = \frac{c}{2\pi\sqrt{\mu_r\varepsilon_r}}\sqrt{\left(\frac{\pi}{W_{eff}}\right)^2 + \left(\frac{\pi}{L_{eff}}\right)^2} \quad (1)$$

$$W_{eff} = a - \frac{d_v^2}{0.95p_v}, \quad L_{eff} = b - \frac{d_v^2}{0.95p_v} \quad (2)$$

where f_{110} denotes the eigenmode frequency, ε_r and μ_r are the relative permittivity and permeability of the substrate, respectively, c is the light velocity of free space, a and b are the width and length of the SIW cavity, respectively, and d_v and p_v are the diameter of metalized via holes and center-to-center pitch between two adjacent via holes, respectively. The final dimensions of the SIWC are determined by the optimized S-parameter responses, which give $a = 6.15$ mm and $b = 4.4$ mm.

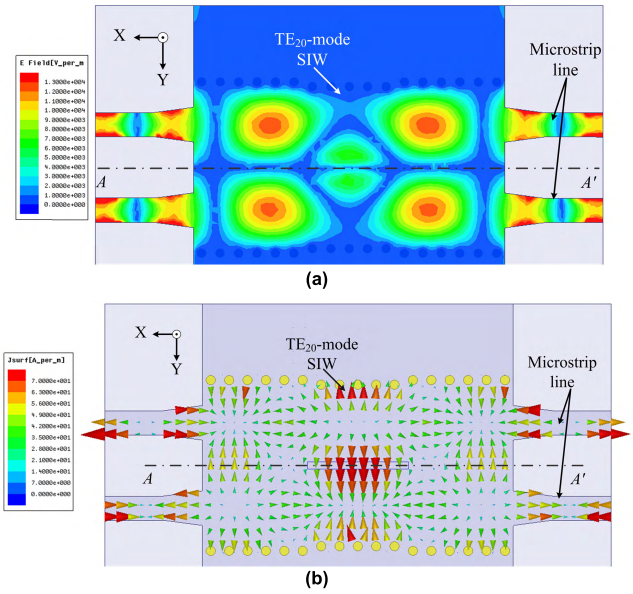

FIGURE 4. (a) The electric field amplitude distribution and (b) the current distribution of TE_{20}-mode SIW and the microstrip lines.

The electric field and current distributions of the TE_{20}-mode SIW and the microstrip lines are shown in Figs. 4(a) and 4(b), respectively. As indicated in Fig. 4, the amplitude distribution of the electric field is symmetric with respect to the *AA'* line, whereas the current distribution shows odd symmetric with respect to the *AA'* line. Therefore, the TE_{20} mode on each side of the SIW can support differential signals with same amplitude and opposite phase.

B. SIMULATED RESULTS

A millimeter-wave SIW four-way anti-phase filtering power divider is designed according to the aforementioned method for operating at 28 GHz. The detailed dimensions are listed in Table 1. Fig. 5(a) shows the simulated S-parameter magnitudes of the filtering power divider. This divider exhibits a fractional bandwidth of 4.8% at 28.17 GHz ranging from 27.49 to 28.85 GHz with the reflection coefficient less than -15 dB. The same S-parameter magnitudes of the four output ports with maximally flat responses are observed due to the symmetric structure. Fig. 5(b) shows the phase responses of the output ports. As indicated, the Port 2 and Port 4 (Port 3 and Port 5) are in-phase and the Port 2 and Port 3 (Port 4 and Port 5) are 180° out of phase. The amplitude and phase imbalances of the output ports are less than 0.2 dB and 180° ±1°, respectively.

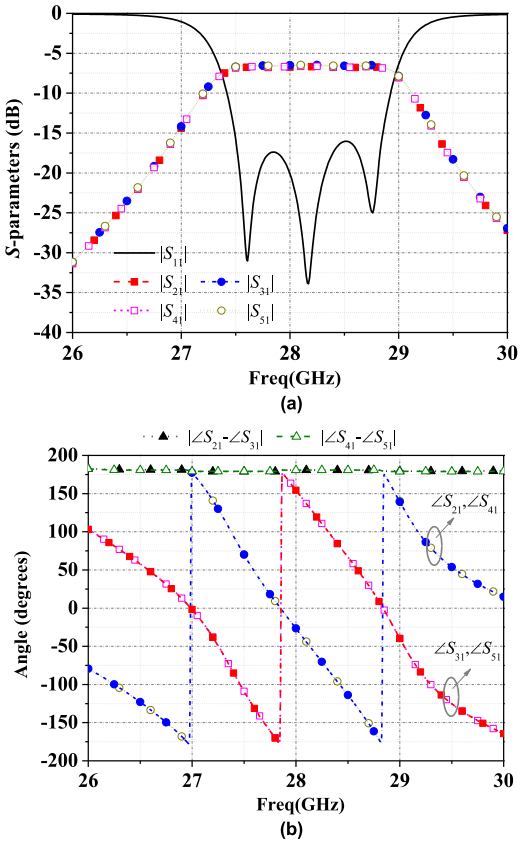

FIGURE 5. Simulated S parameters of the proposed TE_{20}-mode SIW four-way anti-phase filtering power divider: (a) Magnitudes and (b) phase differences between the output ports.

TABLE 1. Dimensions of the filtering power divider (in mm).

Parameter	a	b	g	L_1	L_2	L_3
Value	6.15	4.4	0.2	1.35	3.2	2.65
Parameter	L	p_v	d_v	d	S_w	S_l
Value	2.1	0.8	0.4	1.6	0.3	4.4
Parameter	W_1	W_2	W_m	W_t	L_t	
Value	7.4	7	1.05	1.5	1.7	

III. INTEGRATION DESIGN OF THE MILLIMETER-WAVE FILTERING PATCH ANTENNA ARRAY

A millimeter-wave 1 × 4 TE_{20}-mode SIW dual-slot-fed patch antenna array integrated with the proposed filtering power divider is designed to achieve high selectivity. Two series-fed 1 × 2 sub-arrays are used to construct the 1 × 4 patch antenna array. The filtering power divider is implemented in the center underneath the two sub-arrays, as shown in Fig. 1. The TE_{20}-mode SIW dual-slot-fed patch structure [19], which features wider bandwidth and higher gain than the conventional TE_{10} single-slot-fed patch antennas, is adopted in this work. The detailed designs of the 1 × 2 sub-arrays and the 1 × 4 filtering patch antenna array are explained as follows.

A. SERIES-FED 1 × 2 SUB-ARRAY

Figs. 6(a) and 6(b) show the configuration of the proposed 1 × 2 TE_{20}-mode SIW series-fed sub-array, which is designed with two-layer Rogers 4003C ($\varepsilon_r = 3.55$ and $\tan\delta = 0.0029$ at 10 GHz) substrates with a thickness of 0.5 mm. Fig. 6(c) illustrates the current distribution on the dual-slot-fed patch elements with TM_{10}-mode excitation

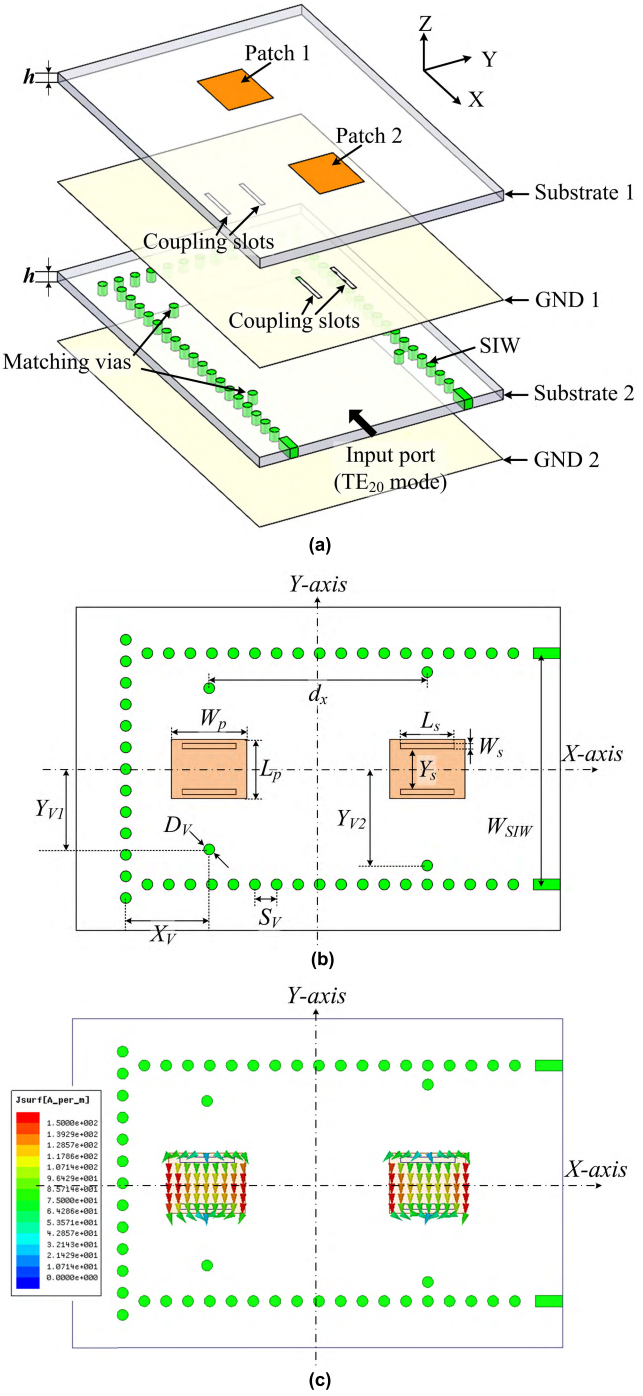

FIGURE 6. Configuration of the TE_{20}-mode SIW series-fed 1 × 2 sub-array with dual-slot-fed patch elements: (a) 3-D view, (b) top view, and (c) current distribution on the dual-slot-fed patch elements.

TABLE 2. Dimensions of The Filtering Powered divider (in mm).

Parameter	W_p	L_p	W_s	L_s	Y_s	X_V
Value	2.8	2.2	0.2	2	1.5	3.1
Parameter	Y_{V1}	Y_{V2}	D_V	S_V	W_{SIW}	d_x
Value	3	3.6	0.4	0.8	8.6	8.1

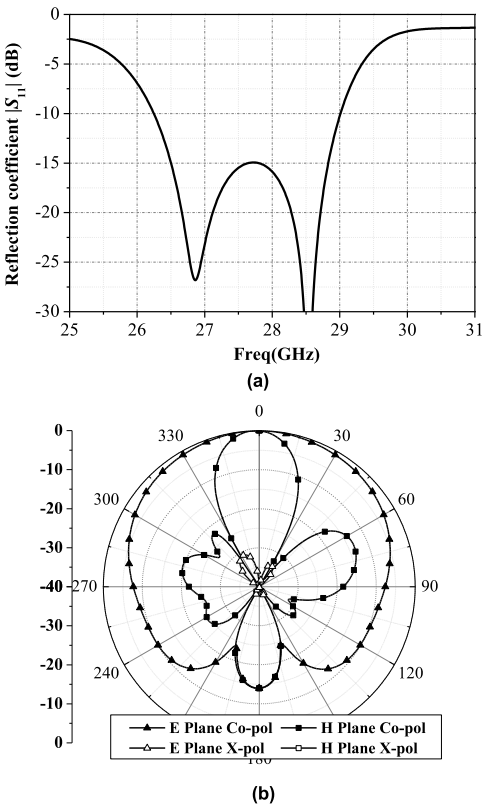

FIGURE 7. Simulated results of the proposed TE_{20}-mode SIW series-fed 1 × 2 sub-array: (a) $|S_{11}|$ and (b) radiation patterns at 28 GHz.

at 28 GHz. The detailed dimensions are listed in Table 2. Fig. 7(a) shows the simulated reflection coefficient $|S_{11}|$ of the 1 × 2 sub-array, which has an impedance bandwidth of 9.95% (26.25−29 GHz) with the reflection coefficient less than −10 dB. The simulated gain at 28 GHz is 12.3 dBi. Fig. 7(b) shows the radiation patterns of the 1 × 2 sub-array at 28 GHz. The E-plane co-polarization radiation pattern is symmetric due to the symmetric dual-slot feeding structure, whereas the peak gain of the H-plane co-polarization radiation pattern is slightly deviated from 0° caused by the series-fed structure. The cross-polarization levels are lower than -30 dB in both E-plane and H-plane.

B. 1 × 4 FILTERING PATCH ANTENNA ARRAY

The integrated 1 × 4 parallel-series-fed filtering patch antenna array is shown in Fig. 1. The overall structure occupies three substrates. The SIW four-way anti-phase filtering power divider provides two-way TE_{20}-mode signals with filtering response, which can be used to excite the series-fed 1 × 2 sub-arrays. In order to improve the deterioration of the H-plane radiation pattern caused by the series-fed structure, two 1 × 2 sub-arrays are mirror-arranged by using a parallel feed with the filtering power divider in the middle underneath them.

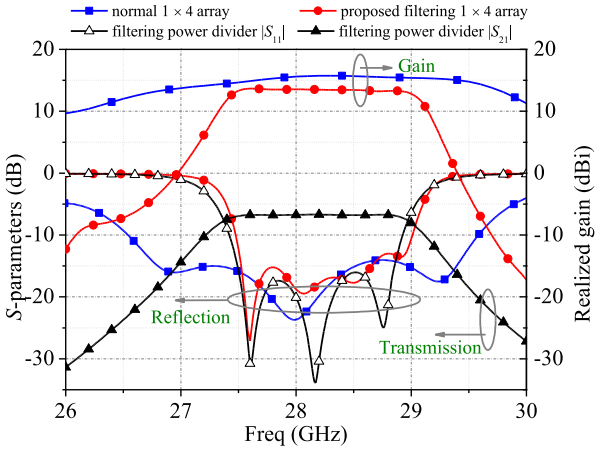

FIGURE 8. Simulated $|S_{11}|$ and gain curves of the proposed filtering 1 × 4 antenna array and a reference 1 × 4 antenna array without the filtering power divider, and the $|S_{11}|$ and $|S_{21}|$ responses of the proposed filtering power divider.

Fig. 8 shows the simulated $|S_{11}|$ responses and gain curves of the proposed filtering 1 × 4 antenna array and a reference 1 × 4 antenna array without the filtering power divider, and the $|S_{11}|$ and $|S_{21}|$ responses of the proposed filtering power divider. As indicated, the gain curve of the proposed filtering antenna array has similar roll-off characteristic to the $|S_{21}|$ response of the proposed filtering power divider, in which the difference of in-band levels between the two curves corresponds to the directivity of the antenna array. A -10-dB impedance bandwidth of 5.4% ranging from 27.48 to 29 GHz is achieved, which is slightly wider than that of the filtering power divider. The peak gain of 13.5 dBi is obtained at 28 GHz. The flat gain curve is observed and the gain variation is less than 0.4 dB in the passband. Fig. 9 shows the simulated radiation patterns at 28 GHz. Due to the symmetric parallel-series feed structure, the 1 × 4 array can achieve symmetric radiation patterns and low cross-polarization levels less than -40 dB in both E-plane and H-plane.

IV. EXPERIMENTAL RESULTS

To verify the design, a prototype of filtering 1 × 4 array was fabricated and measured, as illustrated in Fig. 10. For the cost issue, the proposed three-layer circuits were fabricated individually and then assembled together by screws. A steel support is used to screw the separated circuit boards and the edge-fed SMA connector. The total size is 33 × 27 mm^2.

A. IMPEDANCE BANDWIDTH AND RADIATION GAIN

Fig. 11 shows the simulated and measured broadside gain curves and $|S_{11}|$ responses of the proposed filtering 1 × 4 patch antenna array. The superior reflection coefficient

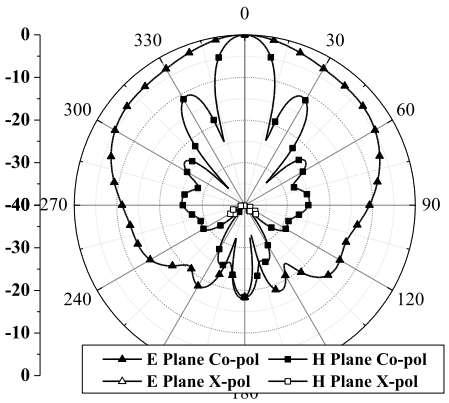

FIGURE 9. Simulated radiation patterns of the proposed 1 × 4 filtering antenna array at 28 GHz.

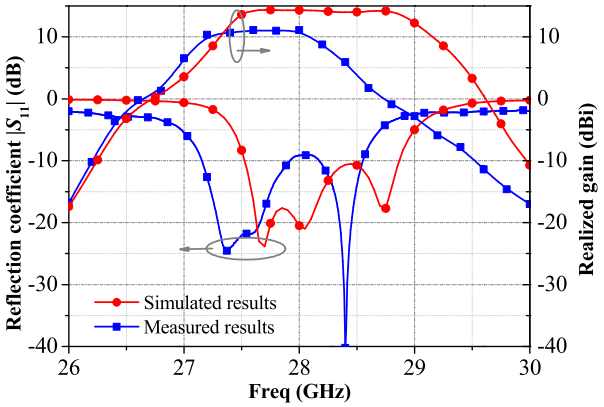

FIGURE 11. Comparison of the measured and simulated gain curves and $|S_{11}|$ responses of the proposed 1 × 4 filtering patch antenna array.

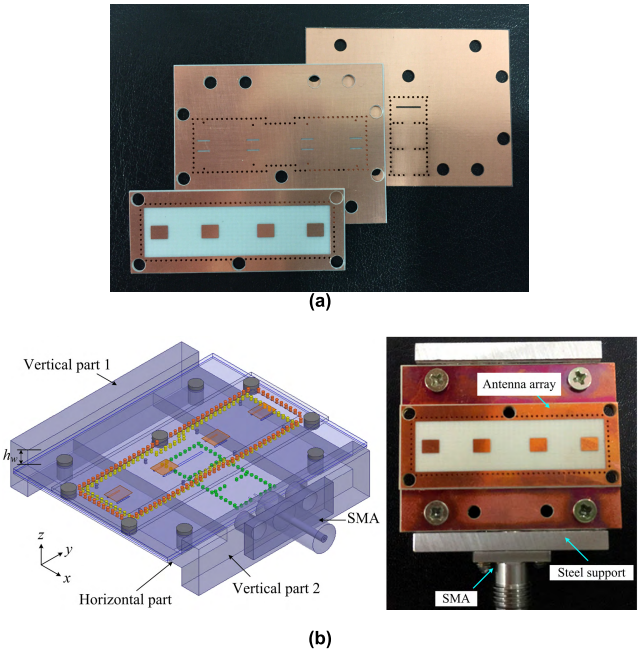

FIGURE 10. Photograph of the fabricated PCB-based 1 × 4 filtering antenna array: (a) Expanded view and (b) assembled view.

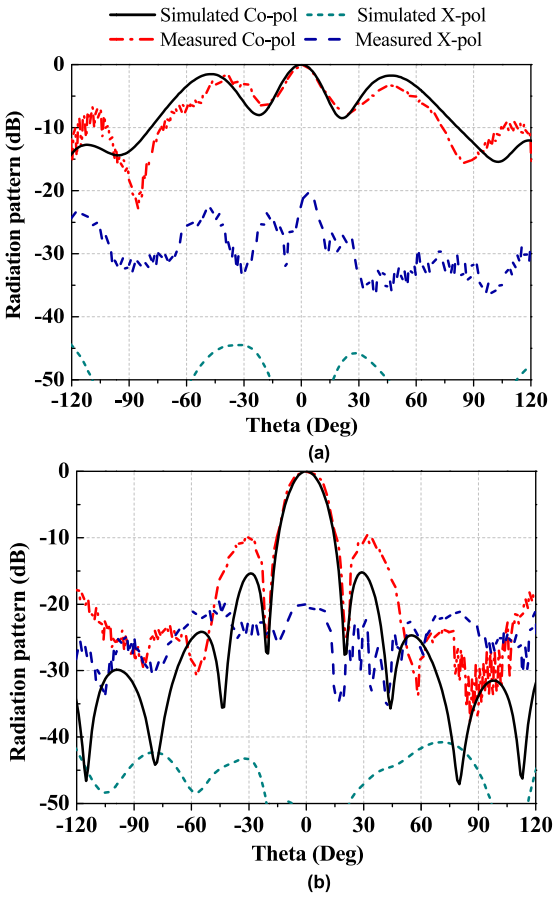

FIGURE 12. Simulated and measured radiation patterns at 28 GHz: (a) E-plane and (b) H-plane.

and high selectivity are achieved around 28 GHz. The measured impedance bandwidth is 5.03% (27.15−28.55 GHz). The measured gain is above 10 dBi from 27.2 to 28 GHz with a peak gain of 11.1 dBi at 27.6 GHz. The in-band gain curve is flat and degrades rapidly in out-of-band with high selectivity. The measured center frequency and bandwidth are slightly decreased from the simulated results due to the possible small air gaps existing between two substrates and the uncertain permittivity of the substrates in millimeter-wave band, which can be improved by adopting accurate multi-layer PCB or LTCC fabrication process with a certain permittivity of substrates.

B. RADIATION PATTERNS

Fig. 12 shows the simulated and measured radiation patterns of the proposed filtering 1 × 4 array at 28 GHz. Owing to the symmetric filtering power divider, the radiation patterns of the array are symmetric in both E-plane and H-plane. The measured cross-polarization levels are below −20 dB in both E-plane and H-plane. The deviation in cross-polarization and side-lobe levels from the simulated results is mainly due to the unbalanced steel support and SMA connector and the fabrication tolerance.

TABLE 3. Comparison with previously reported filtering antenna arrays.

Ref.	Freq. (GHz)	Array Size	Impedance Bandwidth (-10 dB)	Type of Feed Network	Peak gain (dBi)	Differential feed network	X-pol. Level	Radiation Patterns	
								E-plane	H-plane
[13]	5	2 × 2	3%	Microstrip	9.6 @5 GHz	No	-21.6 dB	N.A.	Symmetric
[16]	29.25	1 × 4	1.2%	SIW	8.1 @ 29.25 GHz	No	N.A.	Asymmetric	N.A.
[20]	10.27	2 × 2	8.7%	SIW	11.9 @ 10.27 GHz	No	N.A.	Asymmetric	Symmetric
[21]	2.45	1	2.5%	Microstrip	6.85 @ 2.44 GHz	Yes	-12.6 dB	Symmetric	Asymmetric
This Work	**28**	1 × 4	**5.03%**	**SIW**	**11.1 @ 27.6 GHz**	**Yes**	**-20 dB**	**Symmetric**	**Symmetric**

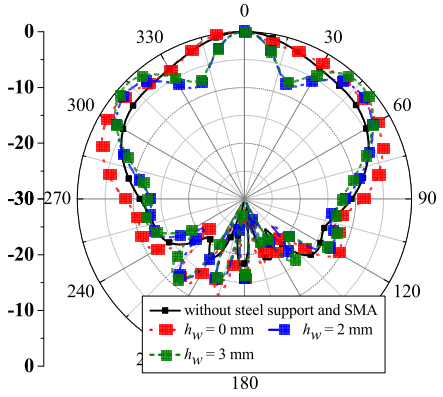

FIGURE 13. Simulated E-plane co-polarization patterns for various h_w.

As shown in Fig. 10(b), the steel support includes horizontal and vertical parts. The two vertical parts behave as two reflected walls lie on the *yz*-plane, which influence the E-plane radiation patterns of the complete antenna array. The height of the vertical parts above the ground is marked as h_w. Fig. 13 shows the impact of h_w on the simulated E-plane co-polarization radiation patterns. As indicated, the side-lobe level increases as h_w increases. When $h_w = 0$ mm, the peak of radiation patterns is slightly shifted from 0° boresight and results in asymmetric radiation pattern. It is mainly caused by the SMA connector even the vertical parts of the steel support are absent. However, all these problems can be further improved by adopting multi-layer PCB fabrication process and low-profile connectors.

Table 3 lists the performance comparison among our work and other published filtering antennas. As indicated, the proposed millimeter-wave filtering antenna array features high gain, differential feed network, low cross polarization, and symmetric radiation patterns in both E-plane and H-plane.

V. CONCLUSION

In this paper, a novel SIW four-way anti-phase filtering power divider is firstly presented, which features symmetric structure, low amplitude and phase imbalances, and high selectivity. Two series-fed 1 × 2 sub-arrays are used to construct the parallel-series-fed 1 × 4 patch antenna array to achieve symmetric radiation patterns in both E-plane and H-plane. The proposed 1 × 4 antenna array can achieve high selectivity, symmetric radiation patterns, and low cross-polarization level in millimeter-wave band.

REFERENCES

[1] D. Chen, L. Zhu, H. Bu, and C. Cheng, "A wideband balun filter on a triple-mode slotline resonator with controllable bandwidth," *IEEE Microw. Wireless Compon. Lett.*, vol. 27, no. 6, pp. 569–571, Jun. 2017.
[2] H. Zhu, A. M. Abbosh, and L. Guo, "Wideband four-way filtering power divider with sharp selectivity and wide stopband using looped coupled-line structures," *IEEE Microw. Wireless Compon. Lett.*, vol. 26, no. 6, pp. 413–415, Jun. 2016.
[3] G. Q. Luo *et al.*, "Filtenna consisting of horn antenna and substrate integrated waveguide cavity FSS," *IEEE Trans. Antennas Propag.*, vol. 55, no. 1, pp. 92–98, Jan. 2007.
[4] X. Y. Zhang, W. Duan, and Y.-M. Pan, "High-gain filtering patch antenna without extra circuit," *IEEE Trans. Antennas Propag.*, vol. 63, no. 12, pp. 5883–5888, Dec. 2015.
[5] F.-C. Chen, J.-F. Chen, Q.-X. Chu, and M. J. Lancaster, "X-band waveguide filtering antenna array with nonuniform feed structure," *IEEE Trans. Microw. Theory Techn.*, vol. 65, no. 12, pp. 4843–4850, Dec. 2017.
[6] H. Chu, C. Jin, J.-X. Chen, and Y.-X. Guo, "A 3-D millimeter-wave filtering antenna with high selectivity and low cross-polarization," *IEEE Trans. Antennas Propag.*, vol. 63, no. 5, pp. 2375–2380, May 2015.
[7] T. Li and X. Gong, "Vertical integration of high-Q filter with circularly polarized patch antenna with enhanced impedance-axial ratio bandwidth," *IEEE Trans. Antennas Propag.*, vol. 66, no. 6, pp. 3119–3128, Jun. 2018.
[8] K. Song, Y. Mo, Q. Xue, and Y. Fan, "Wideband four-way out-of-phase slotline power dividers," *IEEE Trans. Ind. Electron.*, vol. 61, no. 7, pp. 3598–3606, Jul. 2014.
[9] D. S. Eom, J. Byun, and H. Y. Lee, "Multilayer substrate integrated waveguide four-way out-of-phase power divider," *IEEE Trans. Microw. Theory Techn.*, vol. 57, no. 12, pp. 3469–3476, Dec. 2009.
[10] J. Dong, Y. Liu, Z. Yang, H. Peng, and T. Yang, "Broadband millimeter-wave power combiner using compact SIW to waveguide transition," *IEEE Microw. Wireless Compon. Lett.*, vol. 25, no. 9, pp. 567–569, Sep. 2015.
[11] C. Zhu, J. Xu, and W. Wu, "Microstrip four-way reconfigurable single/dual/wideband filtering power divider with tunable frequency, bandwidth and PDR," *IEEE Trans. Ind. Electron.*, vol. 65, no. 11, pp. 8840–8850, Nov. 2018.
[12] X. Zhao, K. Song, Y. Zhu, and Y. Fan, "Wideband four-way filtering power divider with isolation performance using three parallel-coupled lines," *IEEE Microw. Wireless Compon. Lett.*, vol. 27, no. 9, pp. 800–802, Sep. 2017.
[13] C.-K. Lin and S.-J. Chung, "A filtering microstrip antenna array," *IEEE Trans. Microw. Theory Techn.*, vol. 59, no. 11, pp. 2856–2863, Nov. 2011.
[14] Z.-C. Hao, Q. Yuan, B.-W. Li, and G. Q. Luo, "Wideband W-band substrate-integrated waveguide magnetoelectric (ME) dipole array antenna," *IEEE Trans. Antennas Propag.*, vol. 66, no. 6, pp. 3195–3200, Jun. 2018.
[15] K. K. Fan, Z.-C. Hao, Q. Yuan, J. Hu, G. Q. Luo, and W. Hong, "Wideband horizontally polarized omnidirectional antenna with a conical beam for millimeter-wave applications," *IEEE Trans. Antennas Propag.*, vol. 66, no. 9, pp. 4437–4448, Sep. 2018.

[16] H. Chu, J.-X. Chen, S. Luo, and Y.-X. Guo, "A millimeter-wave filtering monopulse antenna array based on substrate integrated waveguide technology," *IEEE Trans. Antennas Propag.*, vol. 64, no. 1, pp. 316–321, Jan. 2016.
[17] H. Y. Jin, K.-S. Chin, W. Q. Che, C.-C. Chang, H.-J. Li, and Q. Xue, "A broadband patch antenna array with planar differential L-shaped feeding structures," *IEEE Antennas Wireless Propag. Lett.*, vol. 14, pp. 127–130, 2015.
[18] Y. Cassivi and K. Wu, "Low cost microwave oscillator using substrate integrated waveguide cavity," *IEEE Microw. Wireless Compon. Lett.*, vol. 13, no. 2, pp. 48–50, Feb. 2003.
[19] H. Jin, W. Che, K. S. Chin, W. Yang, and Q. Xue, "Millimeter-wave TE20-mode SIW dual-slot-fed patch antenna array with a compact differential feeding network," *IEEE Trans. Antennas Propag.*, vol. 66, no. 1, pp. 456–461, Jan. 2018.
[20] Y. Yusuf. H. Cheng, and X. Gong, "Co-designed substrate-integrated waveguide filters with patch antennas," *IET Microw., Antennas Propag.*, vol. 7, no. 7, pp. 493–501, May 2013.
[21] L. Li and G. Liu, "A differential microstrip antenna with filtering response," *IEEE Antennas Wireless Propag. Lett.*, vol. 15, pp. 1983–1986, 2016.

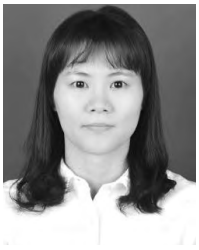

HUAYAN JIN was born in Hangzhou, Zhejiang, China, in 1989. She received the B.S. degree in electronic engineering and the Ph.D. degree in electromagnetic field and microwave technology from the Nanjing University of Science and Technology (NUST), Nanjing, China, in 2011 and 2017, respectively.

From 2012 to 2014, she was an Exchange Student with Chang Gung University, Taoyuan, Taiwan. She is currently a Lecturer with the School of Electronics and Information, Hangzhou Dianzi University, Hangzhou, China. Her main research interests include millimeter-wave antennas, differential-fed antennas, and filtering antennas. She serves as a Reviewer for the IEEE Access, *IET Microwaves, Antennas and Propagation*, IET *Electronics Letters*, and the *International Journal of Electronics*.

GUO QING LUO (M'08) received the B.S. degree from the China University of Geosciences, Wuhan, China, in 2000, the M.S. degree from Northwest Polytechnical University, Xi'an, China, in 2003, and the Ph.D. degree from Southeast University, Nanjing, China, in 2007.

Since 2007, he has been a Lecturer with the Faculty of School of Electronics and Information, Hangzhou Dianzi University, Hangzhou, China, where he was promoted as a Professor, in 2011. From 2013 to 2014, he was with the Department of Electrical, Electronic and Computer Engineering, Heriot-Watt University, Edinburgh, U.K., as a Research Associate, where he was involved in developing low profile antennas for UAV applications. He has authored or coauthored more than 90 technical papers in refereed journals and conferences. He holds 16 patents. His current research interests include RF, microwave and mm-wave passive devices, antennas, and frequency selective surfaces.

Dr. Luo was a recipient of the CST University Publication Award, in 2007, the National Excellent Doctoral Dissertation of China, in 2009, and the National Natural Science Award (Second Class) of China, in 2016. He has served as the Organizing Committee Chair for the 2011 China-Japan Joint Microwave Conference (CJMW 2011), the TPC Chair for the 2017 National Conference on Microwave and Millimeter Waves (NCMMW 2017), and a TPC Chair for the 2018 U.K.-Europe-China Workshop on Millimeter Waves and Terahertz Technologies (UCMMT 2018). He is the Chair of the Hangzhou Chapter, IEEE Microwave Theory and Techniques Society. He also serves a Reviewer for many technical journals, including the IEEE Transactions Antennas Propagation, the IEEE Transactions on Microwave Theory and Techniques, the IEEE Antennas Wireless Propagation Letters, the IEEE Microwave Wireless Component Letters, and the IEEE Access.

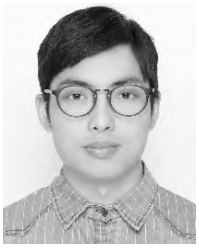

WENLEI WANG received the B.S. degree in electronic information engineering from Hangzhou Dianzi University, Hangzhou, China, in 2017, where he is currently pursuing the the Ph.D. degree in electromagnetic field and microwave technology.

His current research interests include wideband circular polarization filter antenna and millimeter-wave antennas.

WENQUAN CHE (M'01–SM'11) received the B.Sc. degree from the East China Institute of Science and Technology, Nanjing, China, in 1990, the M.Sc. degree from the Nanjing University of Science and Technology (NUST), Nanjing, in 1995, and the Ph.D. degree from the City University of Hong Kong (CITYU), Hong Kong, in 2003.

In 1999, she was a Research Assistant with the City University of Hong Kong. In 2002, she was a Visiting Scholar with the Polytechnique de Montréal, Montréal, QC, Canada. She has been with NUST, from 1995 to 2018, as a Lecturer, Associate Professor, and then a Full Professor. She was the Executive Dean of Elite Education College, NUST, from 2013 to 2018. She is currently a Full Professor with the South China University of Technology. From 2007 to 2008, she has conducted academic research with the Institute of High Frequency Technology, Technische Universität München, Munich, Germany. She was with the City University of Hong Kong, as a Research Fellow and a Visiting Professor, from 2005 to 2006 and from 2009 to 2016, respectively. She has authored or coauthored more than 250 internationally refereed journal papers and more than 100 international conference papers. Her current research interests include microwave and millimeter-wave circuits and systems, microwave monolithic integrated circuits, antenna technologies, and the medical applications of microwave technologies.

Dr. Che is currently an Elected Member of the IEEE MTT-S AdCom, from 2018 to 2020. She was a recipient of the 2007 Humboldt Research Fellowship from the Alexander von Humboldt Foundation of Germany, the fifth China Young Female Scientists Award, in 2008, and the Distinguished Young Scientist Award from the National Natural Science Foundation Committee of China, in 2012. She has been a Reviewer of *IET Microwaves, Antennas and Propagation*. She is currenlty an Associate Editor of the IEEE *Journal of Electromagnetics, RF, and Microwaves in Medicine and Biology*. She is the Editor-in-Chief of the *Microwave and Optical Technology Letters*, from 2019 to 2022. She is a Reviewer of the IEEE Transactions on Microwave Theory and Techniques, the IEEE Transactions on Antennas and Propagation, the IEEE Transactions on Industrial Electronics, and the IEEE Microwave and Wireless Components Letters.

KUO-SHENG CHIN (S'05–M'06–SM'15) received the B.S. degree in electrical engineering from the Chung Cheng Institute of Technology, Taoyuan, Taiwan, in 1986, the M.S.E.E. degree from Syracuse University, Syracuse, NY, USA, in 1993, and the Ph.D. degree in communication engineering from National Chiao Tung University, Hsinchu, Taiwan, in 2005.

From 1986 to 2005, he was with the Chung Shan Institute of Science and Technology, Taoyuan, as a Research Assistant, after becoming an Assistant Scientist, and then an Associate Scientist. He joined Chang Gung University, Taoyuan, in 2006, as a

Faculty Member, where he is currently a Professor with the Department of Electronic Engineering. His current research interests include microwave and millimeter-wave circuits, low-temperature cofired ceramic circuits, array antennas, frequency-selective surfaces, radomes, and electromagnetic pulse research. He was a recipient of the Medal of Excellent Efficiency, the Order of Loyalty and Diligence, the Medal of Outstanding Staff, A Class, and the Medal of Army Achievement, A Class, all from the Ministry of National Defense, Taiwan. He has supervised a student team to win first place in the 2009 National Electromagnetism Application Innovation Competition, Taiwan. He was selected as a recipient of the Outstanding Teaching Award from Chang Gung University, in 2014. He was one of the recipients of the Best Paper Award from the International Conference on Electromagnetic Near Field Characterization and Imaging, in 2009, the Honorable Paper Award from the International High Speed Intelligent Communication Forum, in 2010, the Best Student Paper Award from the International Symposium on Next-Generation Electronics, in 2014, the Best Paper Award from the Taiwan Precision Engineering Workshop, in 2016, and the Best Student Paper Award from the International Symposium on InfoComm and Mechatronics Technology in Bio-Medical and Healthcare Applications, in 2018. He serves as a Reviewer for the IEEE TRANSACTIONS ON MICROWAVE THEORY AND TECHNIQUES, the IEEE TRANSACTIONS ON ANTENNAS AND PROPAGATION, and the IEEE TRANSACTIONS ON COMPONENTS, PACKAGING AND MANUFACTURING TECHNOLOGY.